

STARS

University of Central Florida
STARS

Faculty Bibliography 2000s

Faculty Bibliography

1-1-2003

Defects in m-face GaN films grown by halide vapor phase epitaxy on LiAlO₂

R. R. Vanfleet
University of Central Florida

J. A. Simmons
University of Central Florida

H. P. Maruska

D. W. Hill

M. M. C. Chou

See next page for additional authors

Find similar works at: <https://stars.library.ucf.edu/facultybib2000>

University of Central Florida Libraries <http://library.ucf.edu>

This Article is brought to you for free and open access by the Faculty Bibliography at STARS. It has been accepted for inclusion in Faculty Bibliography 2000s by an authorized administrator of STARS. For more information, please contact STARS@ucf.edu.

Recommended Citation

Vanfleet, R. R.; Simmons, J. A.; Maruska, H. P.; Hill, D. W.; Chou, M. M. C.; and Chai, B. H., "Defects in m-face GaN films grown by halide vapor phase epitaxy on LiAlO₂" (2003). *Faculty Bibliography 2000s*. 4089. <https://stars.library.ucf.edu/facultybib2000/4089>



Authors

R. R. Vanfleet, J. A. Simmons, H. P. Maruska, D. W. Hill, M. M. C. Chou, and B. H. Chai

Defects in *m*-face GaN films grown by halide vapor phase epitaxy on LiAlO₂

Cite as: Appl. Phys. Lett. **83**, 1139 (2003); <https://doi.org/10.1063/1.1599962>

Submitted: 05 March 2003 . Accepted: 06 June 2003 . Published Online: 05 August 2003

R. R. Vanfleet, J. A. Simmons, H. P. Maruska, D. W. Hill, M. M. C. Chou, and B. H. Chai



View Online



Export Citation

ARTICLES YOU MAY BE INTERESTED IN

[Structural characterization of nonpolar \(1120\) a-plane GaN thin films grown on \(1102\) r-plane sapphire](#)

Applied Physics Letters **81**, 469 (2002); <https://doi.org/10.1063/1.1493220>

[Microstructural evolution of a-plane GaN grown on a-plane SiC by metalorganic chemical vapor deposition](#)

Applied Physics Letters **84**, 1281 (2004); <https://doi.org/10.1063/1.1650545>

[Growth of a-plane InN on r-plane sapphire with a GaN buffer by molecular-beam epitaxy](#)

Applied Physics Letters **83**, 1136 (2003); <https://doi.org/10.1063/1.1599634>

Applied Physics Letters

Mid-IR and THz frequency combs
special collection

Read Now!

AIP
Publishing

Defects in *m*-face GaN films grown by halide vapor phase epitaxy on LiAlO₂

R. R. Vanfleet^{a)} and J. A. Simmons

Advanced Materials Processing and Analysis Center (AMPAC) and the Department of Physics, University of Central Florida, Orlando, Florida 32816

H. P. Maruska, D. W. Hill, M. M. C. Chou, and B. H. Chai

Crystal Photonics Inc., 5525 Benchmark Lane, Sanford, Florida 32773

(Received 5 March 2003; accepted 6 June 2003)

Free-standing wafers (50 mm diameter) of GaN were grown by halide vapor phase epitaxy on lattice-matched γ -LiAlO₂. We report a transmission electron microscopy study of defects and defect densities in these wafers. The growth direction is [10 $\bar{1}$ 0]. Stacking faults in the basal plane are seen when viewing the specimen in the [1 $\bar{2}$ 10] direction with an average spacing of less than 100 nm. Convergent beam electron diffraction measurements show no switch in the polarity and thus the faults are proposed to be ABABACAC changes in the stacking. Threading dislocations are found to have a correlated arrangement with a density of $3 \times 10^8 \text{ cm}^{-2}$ when viewing the [1 $\bar{2}$ 10] direction and widely varying (depending upon location) when viewing in the [0001] direction. These dislocations act as “seeds” for postgrowth surface features that directly exhibit the correlated nature of these threading dislocations. © 2003 American Institute of Physics. [DOI: 10.1063/1.1599962]

Nitride-based semiconductor products have burst onto the scene in the last several years, and have now become a major player in the optoelectronics market. Revenues from the use of blue and green light-emitting diodes (LEDs) in the home and commercial lighting business are predicted to reach almost three billion dollars by 2009. Although the blue laser diode (LD) optical storage market is presently still small, it is predicted to reach over the two billion dollar level by 2009. However, continued market growth is in some doubt, because further increases in unit brightness levels for LEDs, which would allow penetration into the illumination industry, may not be possible because the quality of present nitride materials is quite poor. It is difficult to coax even marginal performance levels and operating lifetimes out of the blue LDs, since their structures are filled with deleterious dislocations. Therefore, we have undertaken an effort to prepare low defect density gallium nitride substrates suitable for the homoepitaxial growth of near defect-free device material. We report here our progress in understanding the structural defects which are found in our wafers.

We have used Czochralski grown¹ γ -LiAlO₂ as a starting substrate for GaN growth. γ -LiAlO₂ has an unusual crystal structure consisting of tetrahedra which share edges as well as vertices.² Although the unit cell has square symmetry when looking down the *c* axis, the *a*-*c* (100) plane has the same atomic arrangement as the prismatic face (10 $\bar{1}$ 0) plane of the wurtzite structure. In fact, the *c* parameter of LiAlO₂, 6.268 Å, is close to 2 times $a_h = 6.378$ Å for GaN, while the *a* parameter of LiAlO₂, 5.168 Å, is basically a perfect match to $c_h = 5.165$ Å for GaN. In addition, the GaN hexagonal cell will be oriented sideways, with the polar c_h axis in the plane of growth, which will have profound effects on polarization issues (Fig. 1). In 1998, Ke *et al.*, deposited GaN films³ featuring the (10 $\bar{1}$ 0) orientation⁴ by

metalorganic vapor phase epitaxy (MOVPE) on polished γ -LiAlO₂. We note that conventional growth of GaN on (0001) sapphire substrates gives material with a permanent electric dipole along the *c* axis, leading to the quantum confined Stark effect in GaN quantum well structures.⁵ This internal electric field leads to spatially indirect optical transitions for UV-emitting LEDs, creating much dimmer devices. It was recently demonstrated that growth of GaN on (100) LiAlO₂ gives films with the (10 $\bar{1}$ 0) orientation and, hence brighter emission levels.^{6,7} Recent work using (1 $\bar{1}$ 02) sapphire has renewed interest in placing the *c*, axis in the plane of GaN which has the (11 $\bar{2}$ 0) orientation.⁸

In recent years, a number of researchers have pursued halide vapor phase epitaxy (HVPE) as a quasibulk technique for the growth of thick (>20 μm), large-area GaN substrates.^{9–11} Growth rates in the HVPE machines were very fast, ranging as high as 200 $\mu\text{m/h}$ (3–4 $\mu\text{m/min}$).¹² The thick layer growth is facilitated by the near-equilibrium nature of the process, which can be exploited to generate material with somewhat lower defect densities than other methods.

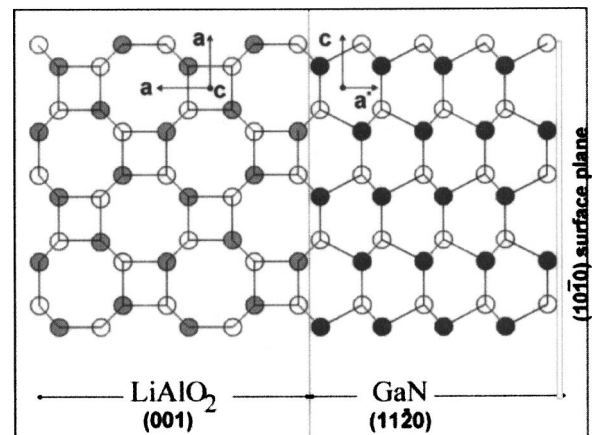


FIG. 1. Atomic arrangement at the interface between LiAlO₂ and GaN.

^{a)}Electronic mail: vanfleet@physics.ucf.edu

Following established practices, Crystal Photonics has designed and constructed a HVPE reactor for the rapid growth of GaN films. The prepared LiAlO₂ wafer is mounted on a SiC-coated graphite chuck. The three furnace zones are typically set at 875–875–850 °C. Nitrogen is set to flow through all gas lines, except for the GaCl generation tube, in which hydrogen flows. The chuck is spun at 60 rpm, the ammonia flowrate is 1 slm, and the HCl flowrate is 20 sccm. A run usually proceeds for 6 h. The growth rate is about 50 μm/h. The GaN wafers are at least 300 μm thick. The resulting wafer has the GaN *c* axis in the plane of the wafer and parallel to the *a* axis of the LiAlO₂ as expected. The [10 $\bar{1}$ 0] GaN direction is normal to the wafer. Many analytical procedures have been undertaken in order to understand the characteristics of these wafers. Results based on a transmission electron microscopy (TEM) study will be presented herein.

TEM specimens were prepared using the focused ion beam (FIB) *ex situ* liftout method.¹³ In this method, the FIB gallium ion beam is used to form and cut free a thin sliver from a specific site of the specimen. This sliver is approximately 20 μm long by 5 μm deep by ~500 nm thick. A micromanipulator is then used to remove the specimen and place it on a carbon film for TEM observation. The Ga ion beam creates a Ga implanted amorphized layer on the surface along with redeposited material that at times obscures areas of the final specimen. The abundance of these redeposited features depends upon the details of the FIB processing. Thus, with care and a little bit of luck, good specimens are rapidly produced from specific sites on the wafer.

FIB liftout specimens from the top surface of (10 $\bar{1}$ 0) GaN can of course easily give any direction perpendicular to this [10 $\bar{1}$ 0] normal. Two convenient choices are [0001] and [1 $\bar{2}$ 10] which are looking into the *c* axis and looking perpendicular to the *c*-axis (into the *a*-axis).

TEM results have shown significant variability depending upon location on the wafer, first or last grown surface, and wafer to wafer. However, several features have been widely seen and appear to be consistent across specimens and a range of processing conditions. Threading dislocations are seen that are qualitatively similar to those commonly seen with other samples grown on sapphire. Differing significantly from what is seen on more traditional substrates, we see a significant number of planar defects that we identify as stacking faults. Such stacking faults have also recently been identified for (11 $\bar{2}$ 0) oriented GaN films grown on (1 $\bar{1}$ 02) sapphire substrates.¹⁴

These planar defects are only seen in the [1 $\bar{2}$ 10] specimens. When viewed directly on the [1 $\bar{2}$ 10] axis the defects are not visible, tilting about the [10 $\bar{1}$ 0] growth direction to put the basal planes at a small incline to the viewing direction makes them visible. Figures 2(a) and 2(b) shows an example of these faults. Figure 2(b) shows a region where the thickness of the specimen is increasing from right to left. The single fringe that not only splits into several fringes but increases in apparent width as the thickness is increased is typical of the contrast expected from an inclined planar defect in this approximately two-beam bright field image $g = 10\bar{1}0$. These defects are absolutely parallel to each other and run perpendicular to the *c* direction. The average spacing

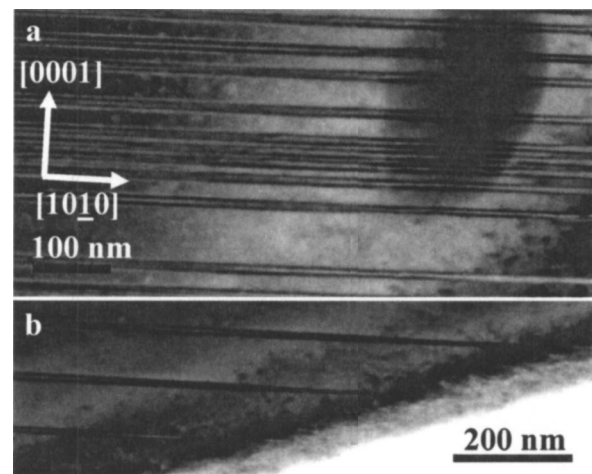


FIG. 2. (a) Stacking faults. (b) Viewed closer in a wedge shaped region.

between these defects is ~100 nm. They are only seen when the *c* axis is tilted relative to the viewing direction and are never seen when the specimen is prepared to look down the *c* axis. This data leads us to identify these as planar defects confined to the basal planes.

The question of stacking fault (with no polarity inversion) versus polar inversion domains is of practical importance. Polar inversion domains have been shown to have different intensities in the $g = 0002$ two-beam imaging conditions due to the underlying nonsymmetry in the crystal structure.¹⁵ We saw no evidence for this contrast mechanism in our specimens. This image contrast is, however, a weaker feature that is usually only suggestive, with more conclusive evidence coming from convergent beam electron diffraction (CBED) methods. CBED is sensitive to the polarity of GaN where an asymmetry in the intensity distribution of the (0002) and (000 $\bar{2}$) diffraction disks is both predicted and seen.¹⁶ However, in the symmetrical orientation of the (0002) peaks required, these defects are not visible. Thus, we tilted the specimen to identify a region with these defects, tilted back to the on-axis condition and performed CBED line scans across the identified region. The asymmetry of the (0002) type peaks was evident, but no evidence for flipping of that asymmetry was seen.

In the *c*-axis direction hexagonal GaN has an ABAB stacking where each A (or B) layer is composed of both Ga and N sublayers with a polarity built in. There is, however, a C site that is equally acceptable and thus an ACAC or BCBC stacking is also possible. There is physically no difference between these variants (shifting the coordinate system will map one into the other) and thus no reason to discuss them unless they are found in the same specimen as we are suggesting here. We propose to identify our observed planar defects as stacking faults between these variants with an ABABACAC stacking. They are thus atomically sharp planar defects that would be invisible if seen edge on. There is no change in the polarity and no extended strain field, consistent with our observations.

GaN when viewed down the *c* axis has a hexagonal symmetry with each of the hexagonal faces being $\langle 10\bar{1}0 \rangle$ directions. Thus, each new nucleation site on LiAlO₂ can begin with any one of these six faces as the growth direction as well as in principle either orientation of the *c* axis. Uniform

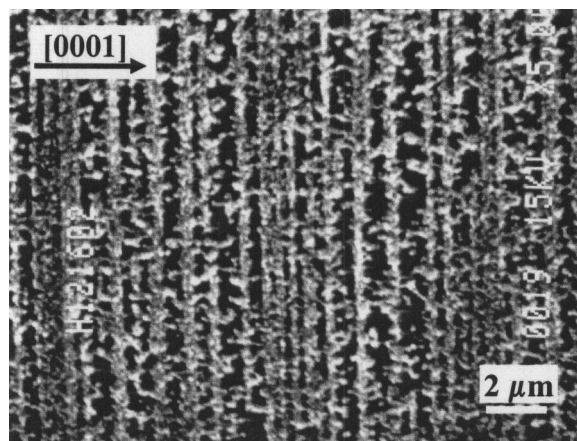


FIG. 3. SEM image of surface features.

alignment of “arrowhead” features on the final wafer surface¹⁷ and the lack of observed inversion domains imply LiAlO₂ is able to fix the *c*-axis direction and suppress inversion domain formation. The six $\langle 10\bar{1}0 \rangle$ directions are not all identical if seen in the same crystal. Three of those faces would give ABAB stacking and the other three ACAC stacking. This suggests random nucleation of the various $\langle 10\bar{1}0 \rangle$ directions as a mechanism for the proposed stacking fault formation.

Scanning electron microscopy (SEM) studies of the final growth surface of these wafers show regions with “plowed field” features as shown in Fig. 3. These surface features consistently match with crystal orientation with the stripes running parallel to the (0002) planes. Our TEM studies have shown these surface features to be polycrystalline GaN that has “seeded” or decorated subsurface features. Figure 4 shows a TEM image of a $[1\bar{2}10]$ specimen (looking along the rows) illustrating one of these surface features associated with a threading dislocation. This implies that the threading dislocations are correlated and predominantly confined to lines that run perpendicular to the *c* axis. The initial nucleation of these correlated dislocations has not been seen and is not understood. However, once formed they would be confined to move only perpendicular to the *c* axis by the ob-

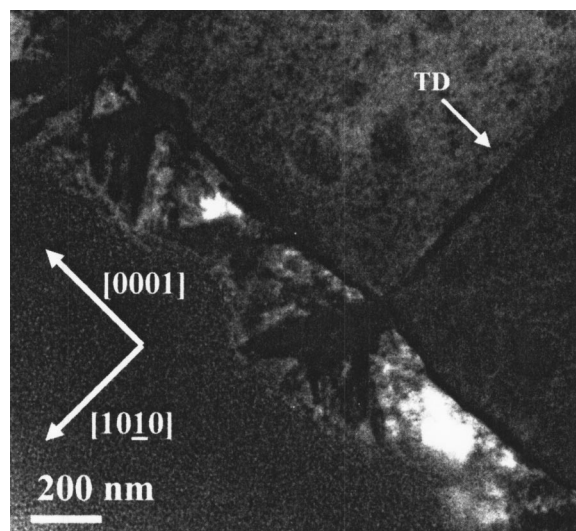


FIG. 4. Cross section showing surface features and their correlation with threading dislocations.

served stacking faults. A further manuscript to discuss the dislocations and their exact nature is in process.

Because the positions of these dislocations are correlated, the exact location and direction in which they are viewed is important. When viewing along the rows ($[1\bar{2}10]$ direction) we expect to see dislocations that match the linear density of the rows. TEM estimates give 1.3×10^4 dislocations/cm in reasonable agreement with SEM results of 1.6×10^4 rows/cm. The average spacing between rows is $\sim 0.6 \mu\text{m}$. From those TEM images and the approximate thickness, the dislocation density per area is estimated to be $3 \times 10^8 \text{ cm}^{-2}$. TEM specimens are $0.5 \mu\text{m}$ or less in thickness. When looking into the row or in the *c* direction, we expect to get significant variation depending upon where the TEM specimen was extracted. If the specimen is from a row, then we would expect to see a higher dislocation density than if the specimen is between the rows. When looking in the *c* direction, with specimens from the plowed field regions, we have seen dislocation counts as high as 10^9 cm^{-2} to lower than 10^7 cm^{-2} .

We have observed by TEM GaN grown on LiAlO₂ with the *c* axis in the plane of the specimen and the $(10\bar{1}0)$ growth normal. Basal plane stacking faults are seen throughout with approximate spacing of 100 nm. Threading dislocations are seen that are correlated in their positioning, occurring in rows that are spaced $\sim 0.6 \mu\text{m}$ apart.

Note added in proof. Recently, Sun *et al.* have discussed stacking faults in M-plane GaN films grown by MBE on LiAlO₂.¹⁸

This work was partially supported by DARPA MTO under the SUVOS program with Joseph Lorenzo of Air Force Research lab as technical monitor.

¹B. Cockayne and B. Lent, *J. Cryst. Growth* **54**, 546 (1981).

²M. Marezio, *Acta Crystallogr.* **19**, 396 (1965).

³X. Ke, X. Jun, D. Peizhen, Z. Yongzong, Z. Guoqing, Q. Rongsheng, and F. Zujie, *J. Cryst. Growth* **193**, 127 (1998).

⁴K. Xu, J. Xu, P. Deng, R. Qiu, and Z. Fang, *Phys. Status Solidi A* **176**, 589 (1999).

⁵P. Lefebvre, B. Gil, J. Allegre, H. Mathieu, N. Grandjean, M. Leroux, J. Massies, and P. Bigenwald, *MRS Internet J. Nitride Semicond. Res.* **4S1**, G3 (1999).

⁶P. Waltereit, O. Brandt, M. Ramsteiner, A. Trampert, H. T. Grahn, J. Menninger, M. Reiche, R. Uecker, P. Reiche, and K. H. Ploog, *Phys. Status Solidi A* **180**, 133 (2000).

⁷E. Kuokstis, C. Q. Chen, M. E. Gaevski, W. H. Sun, J. W. Simin, M. Asif Khan, H. P. Maruska, D. W. Hill, M. M. C. Chou, J. J. Gallagher, and B. Chai, *Appl. Phys. Lett.* **81**, 4130 (2002).

⁸M. D. Craven, S. H. Lim, F. Wu, J. S. Speck, and S. P. DenBaars, *Phys. Status Solidi A* **194**, 541 (2002).

⁹T. Detchprohm, K. Hiramatsu, H. Amano, and I. Akasaki, *Appl. Phys. Lett.* **61**, 2688 (1992).

¹⁰R. J. Molnar, K. B. Nichols, P. Maki, E. R. Brown, and I. Melngailis, *Mater. Res. Soc. Symp. Proc.* **378**, 479 (1995).

¹¹N. R. Perkins, M. N. Horton, and T. F. Kuech, *Mater. Res. Soc. Symp. Proc.* **395**, 243 (1996).

¹²M. Ilegems, *J. Cryst. Growth* **13/14**, 360 (1972).

¹³L. A. Giannuzzi and F. A. Stevie, *Micron* **30**, 197 (1999).

¹⁴M. D. Craven, S. H. Lim, J. S. Speck, *J. Appl. Phys.* (to be published).

¹⁵J. L. Rouviere, M. Arlery, B. Daudin, G. Feuillet, and O. Briot, *Mater. Sci. Eng., B* **50**, 61 (1997).

¹⁶B. Daudin, J. L. Rouviere, and M. Arlery, *Appl. Phys. Lett.* **69**, 2480 (1996).

¹⁷H. P. Maruska, D. W. Hill, M. M. C. Chou, J. J. Gallagher, and B. Chai, *Opto-Electron. Rev.* **11**, 7 (2003).

¹⁸Sun, O. Brandt, U. Jahn, T. Y. Liu, A. Trampert, S. Cronenberg, S. Dhar, K. H. Ploog, *J. Appl. Phys.* **92**, 5714 (2002).